Tree Physiology 33, 684–694
doi:10.1093/treephys/tpt050

Research paper

The evolution and function of vessel and pit characters with respect to cavitation resistance across 10 *Prunus* species

Alexander Scholz[1†], David Rabaey[2†], Anke Stein[1,5], Hervé Cochard[3], Erik Smets[2,4] and Steven Jansen[1,6]

[1]Institute for Systematic Botany and Ecology, Ulm University, Albert-Einstein-Allee 11, D-89081 Ulm, Germany; [2]Section Ecology, Evolution and Biodiversity Conservation, KU Leuven, Kasteelpark Arenberg 31 Box 2437, BE-3001 Leuven, Belgium; [3]INRA, UMR 547 PIAF, F-63100 Clermont-Ferrand, France; [4]Netherlands Center for Biodiversity Naturalis (Section NHN), Leiden University, PO Box 9514, NL-2300 RA Leiden, The Netherlands; [5]Current address: Biodiversity, Macroecology & Conservation Biogeography Group, Faculty of Forest Sciences and Forest Ecology, University of Göttingen, Büsgenweg 2, 37077 Göttingen, Germany; [6]Corresponding author (steven.jansen@uni-ulm.de)

Received October 23, 2012; accepted June 18, 2013; handling Editor Frederick Meinzer

Various structure–function relationships regarding drought-induced cavitation resistance of secondary xylem have been postulated. These hypotheses were tested on wood of 10 *Prunus* species showing a range in P_{50} (i.e., the pressure corresponding to 50% loss of hydraulic conductivity) from −3.54 to −6.27 MPa. Hydraulically relevant wood characters were quantified using light and electron microscopy. A phylogenetic tree was constructed to investigate evolutionary correlations using a phylogenetically independent contrast (PIC) analysis. Vessel-grouping characters were found to be most informative in explaining interspecific variation in P_{50}, with cavitation-resistant species showing more solitary vessels than less resistant species. Co-evolution between vessel-grouping indices and P_{50} was reported. P_{50} was weakly correlated with the shape of the intervessel pit aperture, but not with the total intervessel pit membrane area per vessel. A negative correlation was found between P_{50} and intervessel pit membrane thickness, but this relationship was not supported by the PIC analysis. Cavitation resistance has co-evolved with vessel grouping within *Prunus* and was mainly influenced by the spatial distribution of the vessel network.

Keywords: **bordered pit structure, cavitation resistance, pit membrane, *Prunus*, vessel grouping, wood anatomy.**

Introduction

Plants have developed a hydraulic transport system that relies on water sustaining a tensile force. Since xylem sap is under tension, it is prone to cavitation, i.e., the spontaneous change from liquid to vapor phase (Tyree and Zimmermann 2002). However, drought-induced cavitation is unlikely to happen via homogeneous nucleation and is typically explained based on the air-seeding hypothesis, i.e., aspiration of air into a functional conduit through porous pit membranes between neighboring cell walls (Lens et al. 2013). Since water supply to the leaves is essential for stomatal conductance and photosynthesis, vulnerability to xylem cavitation has been shown to have an important constraint on plant growth and survival (Rood et al. 2000, Davis et al. 2002, McDowell et al. 2008, Brodribb and Cochard 2009, Brodribb et al. 2010). Cavitation resistance is generally quantified by determining P_{50} values, i.e., the pressure corresponding to 50% loss of hydraulic conductivity. The availability of P_{50} values for an increasing number of species (Delzon et al. 2010, Pittermann et al. 2010) in combination with fast acquisition techniques (Cochard et al. 2005) provides new opportunities for (i) understanding the evolutionary forces behind cavitation resistance in a broad range of plant groups (Maherali et al. 2004, Bhaskar et al. 2007, Pittermann et al. 2010, Choat et al. 2012), (ii) unravelling the genetic background of cavitation resistance at an intraspecific level (Lamy et al. 2011, Wortemann et al. 2011) and (iii) increasing our knowledge of structure–function tradeoffs across environmental gradients (Choat et al. 2007).

†AS and DR contributed equally to this study and are both considered as first authors.

Over the last few decades, various studies contributed to our understanding of how anatomical features scale to hydraulic efficiency and safety in angiosperms (Carlquist 1980, 2001, Sperry 2003, Sperry et al. 2005, Hacke et al. 2006). Most previous studies included quantitative features such as vessel diameter, vessel element length and vessel density, while total vessel length and spatial vessel distribution have been quantified in relatively few studies (Loepfe et al. 2007, Schenk et al. 2008, Martínez-Cabrera et al. 2009, Mencuccini et al. 2010, Brodersen et al. 2011, Jansen et al. 2011). Nevertheless, a clear evidence for a vessel-grouping hypothesis has been postulated by Carlquist (1984, 2009), who states that high vessel grouping (i.e., average number of vessels contacting a vessel) is more pronounced in xeric-adapted species with a non-conductive ground tissue as compared with their relatives in more mesic environments. The functional explanation for this finding is that large vessel groups contribute to bypassing the more frequent embolisms in dry environments (Carlquist 2009). In contrast, theoretical insights into the three-dimensional vessel network suggest that high vessel connectivity decreases resistance to cavitation by increasing the probability for the spread of embolism via air-seeding (Loepfe et al. 2007, Martínez-Vilalta et al. 2012). The latter authors applied novel parameters to quantify vessel connectivity (i.e., the spatial distribution of vessels) instead of Carlquist's vessel-grouping index (Mencuccini et al. 2010).

In addition, several studies highlighted the importance of the bordered pit structure with respect to hydraulic resistance and cavitation resistance (Tyree and Sperry 1989, Choat et al. 2008, Hacke and Jansen 2009). Wheeler et al. (2005) found solid evidence in Rosaceae for the 'rare pit' hypothesis, suggesting a positive correlation between the average intervessel pit area per vessel (A_P) and P_{50}. This means that vulnerability to cavitation depends on the number of pits between vessel elements, assuming that a high number of intervessel pits increases the likelihood of a single large pit membrane pore that triggers air-seeding (Choat et al. 2003). Further evidence for this hypothesis was found for a broader sampling across angiosperms (Hacke et al. 2006, 2007, 2009, Sperry et al. 2007, Christman et al. 2012).

Lens et al. (2011) provided empirical evidence for the vessel-grouping hypothesis of Carlquist (1984), suggesting that cavitation-resistant species of *Acer* show higher vessel grouping as compared with species that are less cavitation resistant. Although at first sight Carlquist's vessel-grouping hypothesis seems to contradict the rare pit hypothesis, Lens et al. (2011) illustrated that quantitative differences in vessel grouping were compensated by vessel diameter and vessel length, resulting in smaller vessel wall areas in cavitation-resistant species, but constant values for A_P (the total intervessel pit membrane area per vessel) across seven *Acer* species.

To clarify the uncertainties about wood anatomical features associated with cavitation resistance, especially vessel grouping and pit quality and quantity, this paper focuses on 10 species of the genus *Prunus*. The species selected show P_{50} values ranging from −3.54 MPa in *Prunus padus* L. to −6.27 MPa in *Prunus cerasifera* Ehrh. as reported by Cochard et al. (2008). Although some anatomical data for these species had already been measured by the latter authors, our intention was to explore functional trends based on more measurements and a larger set of vessel and pit characteristics, using various microscope techniques. Given that *Prunus* belongs to the Rosaceae family, from which 11 species out of eight genera were included in the study by Wheeler et al. (2005), we expected that the total intervessel pit membrane area per vessel (A_P) would be associated with P_{50} according to the rare pit hypothesis. By performing a phylogenetically independent contrast (PIC) analysis, we also aim to test the hypothesis that xylem anatomical characters that determine cavitation resistance in *Prunus* have co-evolved together with P_{50} due to adaptive association (Bhaskar et al. 2007, Hacke et al. 2009, Pittermann et al. 2010). We therefore hypothesize that closely related species share similar adaptations to cavitation resistance.

Materials and methods

Plant materials

Plant materials included four wild and six cultivated species of *Prunus* that were previously investigated by Cochard et al. (2008). *Prunus padus* was collected on a humid site in the Auvergne Volcano Park, while *Prunus avium* (L.) L. and *Prunus spinosa* L. were from a mesophilic site in this park. *Prunus mahaleb* L. was the only species growing on a xerophilic site in the Limagne valley. All other species (*Prunus cerasifera, P. cerasus* L., *P. persica* (L.) Batsch, *P. domestica* L., *P. armeniaca* L. and *P. dulcis* (Mill.) Rchb.) were from mesophilic sites in the same area. To guarantee a direct link between pit morphology and cavitation resistance, most pit characters were based on anatomical measurements of the same branches studied by Cochard et al. (2008). Other anatomical measurements, however, were based on five new branches per species, which were collected from the same specimens in January 2010. Because intra-tree variation in P_{50} values of *Prunus* was found to be low (Cochard et al. 2008), combining measurements of two different groups of branches should not bias the link between P_{50} and anatomy.

Special attention was paid to collecting straight branches fully exposed to the sun, with a similar length (c. 1 m) and diameter (5–10 mm) as sampled by Cochard et al. (2008). Fresh material was immediately wrapped in wet tissue, enclosed in plastic bags and sent to Ulm University for anatomical analysis.

P_{50} values were taken from Cochard et al. (2008). Anatomical data from this study, however, were not re-used because of the

higher number of samples measured in the present study and a frequently different definition of anatomical characters.

Light microscopy

Thin sections (15–20 μm) were prepared using a sliding microtome (Reichert, Vienna, Austria). After bleaching with Danklorix bleach and rinsing with water, sections were stained with a mixture of safranin and alcian blue (35 : 65, v/v). They were then dehydrated with an ethanol series (50, 70, 96%) and treated with the clearing agent Parasolve (Prosan, Merelbeke, Belgium). The sections were embedded in Euparal (Agar Scientific Ltd, Essex, UK). Macerated cells were obtained following Franklin (1945) to measure vessel element length (L_{VE}) and fiber length (L_F) based on 50 cells from the last two growth rings.

Light microscopy (LM) observations were carried out with a Dialux 20 (Leitz, Wetzlar, Germany) fitted with an oil immersion objective, and digital pictures were taken with a PixeLINK PL-B622CF camera.

Scanning electron microscopy

Small blocks (c. 3 mm^2) were trimmed with a razor blade, cleaned with Danklorix bleach and attached to stubs using electron-conductive carbon paste. The samples were sputter coated for 3 min with gold (Spi-Supplies, West Chester, PA, USA). Observations were carried out using a Jeol JSM 6360 SEM (Jeol Ltd, Tokyo, Japan) at 15 kV.

Transmission electron microscopy

Two sets of plant material were prepared for transmission electron microscopy (TEM). Since all pit morphological features were based on the material that was used to construct vulnerability curves by Cochard et al. (2008), we prepared these dried samples for TEM using the method provided below. These samples were not re-hydrated before starting the TEM preparation, although at least a partial rehydration by using fixatives and washing with phosphate buffer was expected. In addition, we prepared material from fresh branches that were kept frozen at –20 °C for several months, defrosted and rehydrated under vacuum overnight. The combination of both 'dry' and 'wet' samples allowed us to compare the pit membrane thickness with a differing dehydration status ($T_{PM\ dry}$ and $T_{PM\ wet}$). All pit membrane thickness measurements were conducted on different vessels of a specimen. We were unable to obtain 15 measurements of $T_{PM\ wet}$ for *P. mahaleb* because intervessel walls were extremely difficult to find in the ultrathin sections. However, sufficient measurements were obtained for this species for $T_{PM\ dry}$.

Small segments of 2 mm^3 were fixed in Karnovsky's fixative at room temperature (Karnovsky 1965). After washing in 0.2 M phosphate buffer, the samples were postfixed in 2% buffered osmium tetroxide for 2 h at room temperature, washed and dehydrated through a graded propanol series. The specimens were stained with uranyl acetate in ethanol for 30 min at 37 °C, and rinsed three times with propanol 100%. Propanol was replaced by propylenoxide, which was gradually replaced with Epon resin (Sigma-Aldrich, Steinheim, Germany) at room temperature. The resin was polymerized at 60 °C for 48 h. Embedded samples were trimmed and sectioned with an ultramicrotome (Ultracut E, Reichert-Jung, Austria). Semi-thin sections cut with a glass knife were heat-fixed to glass slides, stained with 0.5% toluidine blue in 0.1 M phosphate buffer and mounted in DPX (Agar Scientific, Stansted, UK). Ultra-thin sections (c. 90 nm) were cut using a diamond knife, attached to 300 mesh copper grids (Agar Scientific, Stansted, UK) and stained manually with lead citrate for 1 min. Observations were carried out using a Zeiss EM 900 microscope (Carl Zeiss AG, Germany) at 80 kV accelerating voltage.

Anatomical measurements

A list of the anatomical features measured is provided in Table 1, including definitions, and acronyms. Detailed information about the number of measurements and how features were quantified is provided in Table S1 available as Supplementary Data at *Tree Physiology* Online. In general, most characters follow Wheeler et al. (2005), Jansen et al. (2011), Lens et al. (2011) and Scholz et al. (2013). All measurements were carried out on images using ImageJ (Rasband 1997).

Because wood of some *Prunus* species shows a tendency toward ring-porosity, the measurements were conducted on ~100 vessels per transverse section, distinguishing earlywood (E_W) from latewood (L_W). A mean value was determined separately for earlywood and latewood vessels, except for diffuse-porous wood.

Vessel length distributions were measured by applying the silicon injection technique (Wheeler et al. 2005, Hacke et al. 2007). Five fresh branches per species with a length of 10–20 cm were first flushed with ultrapure, degassed water at 0.2 MPa for at least 30 min to remove embolism and then injected basipetally with a fluorescent silicon mixture (UVITEX + Rhodorsil ESA7250 A + B, bluesil GmbH) for at least 4 h under 0.2 MPa using a pressure chamber (PMS Instruments, Albany, OR, USA). After 5 h of hardening at 20 °C, the maximum vessel length was determined and stems were sectioned at five different heights calculated after Sperry et al. (2005). Silicon-filled vessels were counted for each section and vessel length distributions were calculated using the exponential decay function of Sperry et al. (2005).

The three dimensional distribution of xylem vessels has been studied at various scales, using different terms for related concepts, such as vessel grouping, aggregation, connectivity, redundancy, sectoriality, integration and segmentation (Martínez-Vilalta et al. 2012). We define the vessel-grouping index following Carlquist (1984) as the total number of vessels divided by the total number of vessel groups (including both

Table 1. List of characters measured with their acronyms, definitions and units.

Acronym	Definition	Units
A_P	Intervessel pit area per vessel = $A_V \times F_P$	mm^2
A_{PIT}	Intervessel pit surface area = area occupied by the pit border or the intervessel pit membrane	μm^2
$A_{PIT\ AP}$	Pit aperture surface area	μm^2
A_V	Vessel surface area = $\pi \times D_{RL} \times L_V$	mm^2
D	Arithmetic vessel diameter = vessel diameter based on the equivalent circle area of a vessel	µm
D_H	Vessel diameter corresponding to average lumen conductivity; $(\sum D^4/N)^{1/4}$	µm
D_{MAX}	Feret's diameter = maximum vessel diameter	µm
$D_{PA\ ratio}$	Ratio of the diameter of the outer pit aperture as measured following the widest ($D_{PA\ long}$) and the shortest ($D_{PA\ short}$) axis	–
F_C	Intervessel contact fraction = portion of vessel wall in contact with other vessels based on transverse sections	–
F_{LC}	Vessel contact length fraction = $L_C/L_V = 1 - V_S$	–
F_P	Pit fraction = fraction of total vessel wall area occupied by intervessel pits = $F_C \times F_{PF}$	–
F_{PF}	Pit-field fraction = fraction of intervessel wall area occupied by intervessel pits	–
L_C	Vessel contact length = average contact length between adjacent vessels = $L_V \times (1 - V_S)$	cm
L_V	Vessel length	cm
L_{VE}	Vessel element length	µm
P_{50}	Cavitation pressure at 50% loss of conductivity	MPa
T_{PM}	Intervessel pit membrane thickness measured at its thickest point	µm
T_{VW}	Intervessel wall thickness measured as the double intervessel wall in the center of adjacent vessels	µm
$T_{VW}\ D_{MAX}^{-1}$	Theoretical vessel implosion resistance	–
V_D	Vessel density = number of vessels per mm^2	mm^{-2}
V_G	Vessel-grouping index = total of vessels divided by total number of vessel groups; a solitary vessel counts as one vessel group	–
V_S	Solitary vessel index = ratio of solitary vessels to total vessel groupings (incl. solitary and grouped vessels)	–

solitary vessels and vessel multiples) as seen in a transverse section. A solitary vessel counts as one vessel group. Intervessel connectivity is interpreted as a broader term that includes vessel and pit characteristics of the overlapping vessel wall area between neighboring (connected) vessels.

Correlation analyses

Depending on the normality of the data, Pearson or Spearman correlation analyses were performed using R (R Core Team 2013) to determine the relationship between wood anatomical features and P_{50}. Correlations were considered significant at $P \leq 0.05$. A post hoc Bonferroni test was applied after generating a correlation matrix. To test for intra-tree variation between branches and interspecific variation, an ANOVA (analysis of variance) was applied to the characters.

Principal component analysis (PCA)

A varimax rotated principal component analysis (PCA) was conducted using SPSS 19 (SPSS Inc., Chicago, IL, USA) for a selection of 12 characters that were found to correlate significantly with P_{50} based on the Spearman or Pearson correlation analysis, or based on previous studies (Wheeler et al. 2005, Christman et al. 2009, Lens et al. 2011). Correlations between the principal component scores and P_{50} were again analyzed using Spearman's rank correlation.

Comparative phylogenetic analysis

Sequences for two markers (ITS and trnL–trnF) from Bortiri et al. (2001) were downloaded from GenBank and aligned using Geneious (Drummond et al. 2011). Maximum likelihood analyses were carried out using the RaxML search algorithm under the GTRGAMMA approximation of rate heterogeneity for each gene (Stamatakis et al. 2005, Stamatakis 2006). Two hundred bootstrap trees were inferred using the RaxML Rapid bootstrap algorithm (ML-BS) to provide support values for the best scoring tree, which was used for comparative phylogenetic analysis.

Phylogenetically independent contrasts

A PIC analysis was conducted to elucidate the impact of phylogeny on our analyses (Felsenstein 1985, Schenk et al. 2008, Pittermann et al. 2010, Zanne et al. 2010). Phylogenetically independent contrast uses phylogenetic information to transform interspecific data into taxa-independent data for further statistical analyses. Phylogenetically independent contrast correlation coefficients and significant levels were determined using the R package Picante (Kembel et al. 2010). The package includes correction algorithms for calculated branch lengths. All branches were unified to one length to minimize type 1 error rate (Ackerly 2000). The phylogenetic contrast for each species node was then calculated.

Results

There was considerable wood anatomical variation among the 10 *Prunus* species, especially in spatial vessel distribution (i.e., vessel-grouping index) and pit membrane thickness (Figure 1). An overview of the anatomical data is provided in

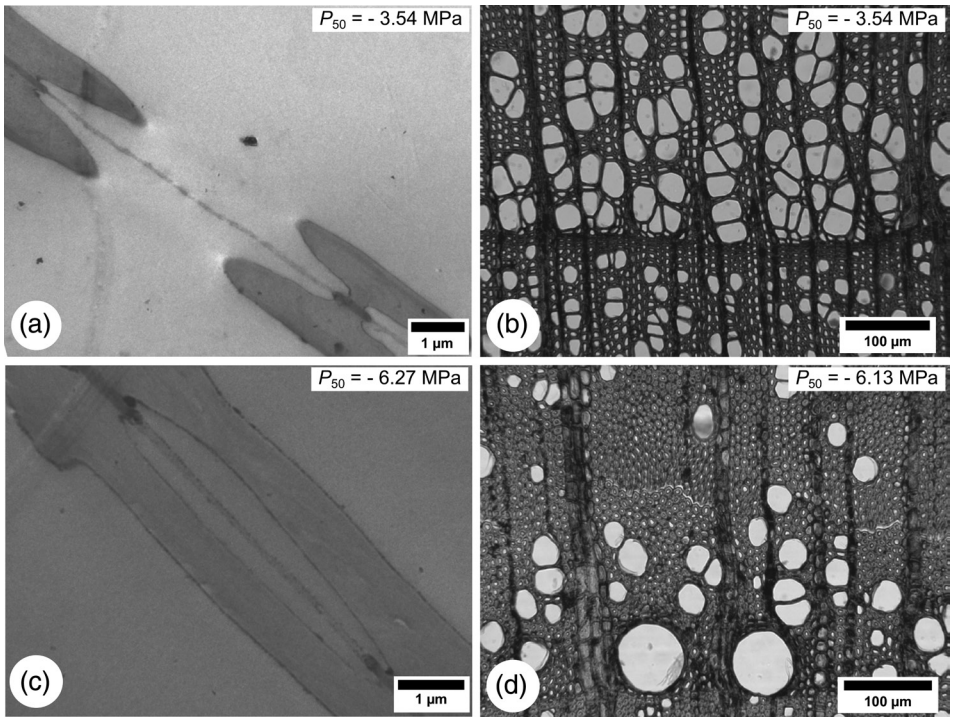

Figure 1. Transverse wood anatomical sections illustrating variation at the pit level and vessel connectivity across three *Prunus* species: (a and b) *P. padus*; (c) *P. cerasifera*; (d) *P. dulcis*. The P_{50} value of each species is indicated in the upper right corner. The TEM images (a and c) demonstrate an increase in pit membrane thickness with increasing cavitation resistance. Light microscopy images (b and d) show variation in vessel diameter, vessel grouping and porosity, with diffuse porous wood in *P. padus* (b) and semi-ring porous wood in *P. dulcis* (d).

Table S2 available as Supplementary Data at *Tree Physiology* Online.

While most species are diffuse-porous, there is a tendency toward ring-porosity in *P. dulcis*, *P. avium* and *P. padus*. The vessel-grouping index (V_G) varied significantly between species (ANOVA, $P < 0.001$, $F = 5.835$, df = 9), with mean values ranging from 2.5 for the least cavitation-resistant species (*P. padus*, $P_{50} = -3.54$ MPa) to 1.2 for *P. mahaleb* ($P_{50} = -5.55$ MPa). Owing to the direct dependency of V_G and the solitary vessel index (V_S), variation in V_S was similar. The contact fraction (F_C) was also significantly variable (ANOVA, $P < 0.001$, $F = 2.14$, df = 9), with the lowest contact fraction in *P. cerasus* ($F_C = 0.04$) and the highest one in *P. spinosa* ($F_C = 0.11$). Vessel density (V_D) ranged from 70 vessels per mm^2 in *P. mahaleb* to 22 in *P. dulcis* and showed a high variability (ANOVA, $P < 0.001$, $F = 6.967$, df = 9). Because vessel density is primarily determined by vessel diameter ($P < 0.001$; $r = 0.46$), a high variability in vessel diameter was found between the species (ANOVA, $P < 0.001$, $F = 4.799$, df = 9).

Although anatomical features were considerably variable within a single tree, with standard deviations up to 25–30%, interspecific differences were larger than the intraspecific variation for all characters measured.

Results of the correlation analysis between P_{50} and wood anatomical characters are presented in Table 2. The vessel-grouping features V_G and V_S had a strong influence on cavitation resistance, with a positive correlation for V_G (Figure 2; $r = 0.81$, $P = 0.004$) and a negative correlation for V_S ($r = -0.78$, $P = 0.008$). Therefore, species with low V_G (*P. dulcis*, *P. armeniaca* and *P. domestica*) were generally more cavitation-resistant than species with high V_G values (*P. padus*, *P. cerasus* and *P. avium*) (see Figure S1 available as Supplementary Data at *Tree Physiology* Online). Vessel contact length fraction (F_{LC}) was also highly correlated with P_{50} ($r = 0.76$, $P = 0.01$). Intervessel pit surface area (A_P) was not correlated with P_{50} ($r = -0.18$, $P = 0.6$), but a correlation with pit fraction (F_P; $r = 0.46$, $P = 0.017$) was found. There was a negative correlation with pit membrane thickness for both dried and wet samples (Figure 3; $T_{PM\ dry}$ $r = -0.75$, $P = 0.01$; $T_{PM\ wet}$ $r = -0.63$, $P = 0.06$). Interestingly, pit membranes in fresh (i.e., wet) samples were on average 1.44 (±0.25) times thicker than the pit membranes in dried wood samples (Figures 3 and 4). An exception, however, was found for *P. domestica*. In general, dried pit membranes appeared electron dense, while hydrated pit membranes were transparent with very fine, electron-dense dots in their matrix (Figure 4a). The variation in pit membrane thickness was also larger in wet samples compared with dried samples, spanning a range of 130 and 87 nm. There was a weak correlation with pit aperture shape ($D_{PA\ ratio}$; $r = -0.60$, $P = 0.068$), and a weak trend for cavitation-resistant species to have longer vessels (L_V; $r = -0.56$, $P = 0.09$). Other wood anatomical features, including double intervessel wall thickness (T_{VW}), were not correlated with P_{50}.

Table 2. Pearson or Spearman correlations and PIC correlations for relationships between P_{50} and the wood anatomical characters measured across 10 *Prunus* species. Bold values indicate a significant ($P < 0.05$) correlation. Acronyms of characters are given in Table 1. *Prunus mahaleb* was excluded for $T_{PM\ wet}$.

	Pearson or Spearman correlation		PIC correlation	
Character	*r*	*P* value	*r*	*P* value
A_P	−0.18	0.600	0.0023	0.900
A_{PIT}	0.28	0.420	0.05	0.560
$A_{PIT\ AP}$	−0.09	0.791	0.03	0.610
A_V	−0.46	0.171	−0.54	0.100
D	−0.13	0.705	0.04	0.580
D_H	−0.12	0.727	0.002	0.910
D_{MAX}	−0.03	0.919	0.11	0.350
$D_{PA\ ratio}$	−0.60	0.068	0.26	0.130
F_C	0.29	0.410	0.417	0.250
F_{LC}	**0.76**	**0.010**	**0.67**	**0.004**
F_P	**0.46**	**0.017**	0.18	0.220
F_{PF}	0.43	0.209	**0.71**	**0.002**
L_C	0.07	0.836	0.16	0.250
L_V	−0.56	0.090	0.09	0.400
L_{VE}	−0.15	0.668	0.12	0.320
$T_{PM\ dry}$	**− 0.75**	**0.012**	0.29	0.110
$T_{PM\ wet}$	−0.63	0.066	0.22	0.170
T_{VW}	0.10	0.765	0.26	0.140
$T_{VW}\ D_{MAX}^{-1}$	−0.18	0.580	0.15	0.260
V_D	0.16	0.650	0.02	0.710
V_G	**0.81**	**0.004**	**0.60**	**0.008**
V_S	**− 0.78**	**0.008**	**0.67**	**0.004**

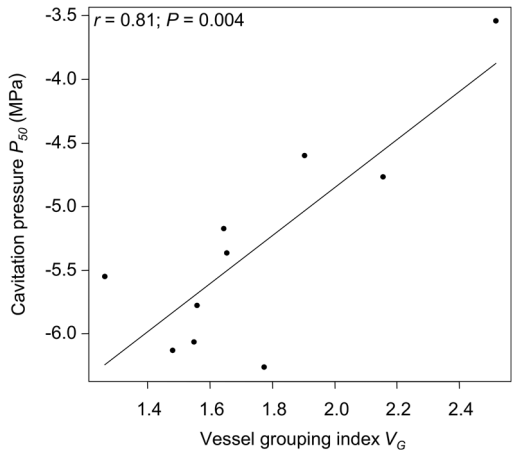

Figure 2. Relationship between cavitation resistance (P_{50}) and vessel-grouping index (V_G) across 10 *Prunus* species.

Possible interactions between the characters investigated were tested using a PCA (Figure 5). Twelve of the most important characters with high correlation coefficients were selected (Table 3). All components with an eigenvalue above 1 were retained. This resulted in four components explaining 90.03% of the total variance. Only PC4 ($P = 0.01$), which included the vessel-grouping indices V_G and V_S, was strongly correlated

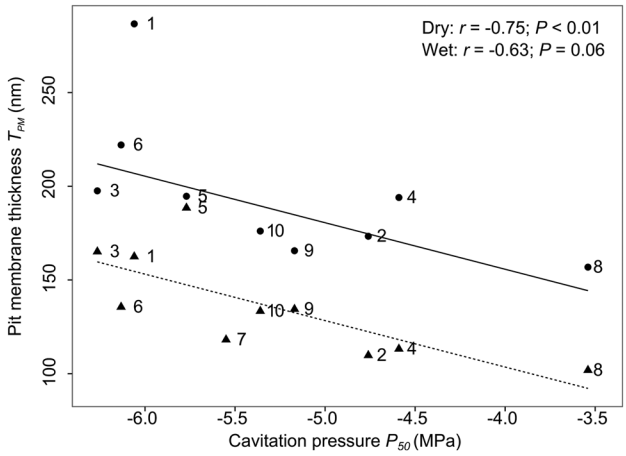

Figure 3. Relationship between cavitation resistance (P_{50}) and pit membrane thickness for the *Prunus* species. Fresh (i.e., hydrated) pit membranes ($T_{PM\ wet}$, n = 9 species, solid line, black dots) were on average 1.44 (±0.25) times thicker than air-dried samples ($T_{PM\ dry}$, n = 10 species, dashed line, triangles). Only a small difference between $T_{PM\ wet}$ and $T_{PM\ dry}$, however, was found for *P. domestica*. 1 = *P. armeniaca*, 2 = *P. avium*, 3 = *P. cerasifera*, 4 = *P. cerasus*, 5 = *P. domestica*, 6 = *P. dulcis*, 7 = *P. mahaleb*, 8 = *P. padus*, 9 = *P. persica*, 10 = *P. spinosa*.

with P_{50} and explained 8.3% of the variance. All other principal components were not correlated with P_{50}.

Two major clades (A and B) could be distinguished in the reconstructed phylogeny (Figure 6). While clade B included species with P_{50} values ranging from −3.54 to −5.55 MPa, clade A contained the most cavitation-resistant species with P_{50} values ranging from −5.18 to −6.26 MPa. The PIC analysis revealed trends between P_{50} and wood anatomical characters that were in line with the correlation matrix (Table 2): V_G (Figure 7b), V_S and F_{LC} showed equally significant *r*-values (Table 2). However, F_{PF} was only correlated with P_{50} in the PIC analysis ($r = 0.71$, $P = 0.002$), while the correlations between P_{50} and $T_{PM\ dry}$ (Figure 7a, $r = 0.43$, $P = 0.209$), $T_{PM\ wet}$ and F_P were not supported by PIC.

Discussion

Our results demonstrate that vessel grouping and some pit characteristics play an important role in determining P_{50} across 10 *Prunus* species. Species with high cavitation resistance show mainly solitary vessels, while high vessel grouping was more common in species with less negative P_{50} values. The vessel-grouping index (V_G, $r = 0.81$, $P = 0.004$), the solitary vessel index (V_S, $r = -0.78$, $P = 0.008$) and the vessel contact length fraction (F_{LC}, $r = 0.76$, $P = 0.01$) were highly correlated with P_{50}. Results from the PCA analysis confirmed that vessel dimensions and vessel-grouping characters contribute significantly to variation in P_{50}. These findings are in agreement with the hydraulic model of Loepfe et al. (2007), which was further developed by Martínez-Vilalta et al. (2012) based on vessel

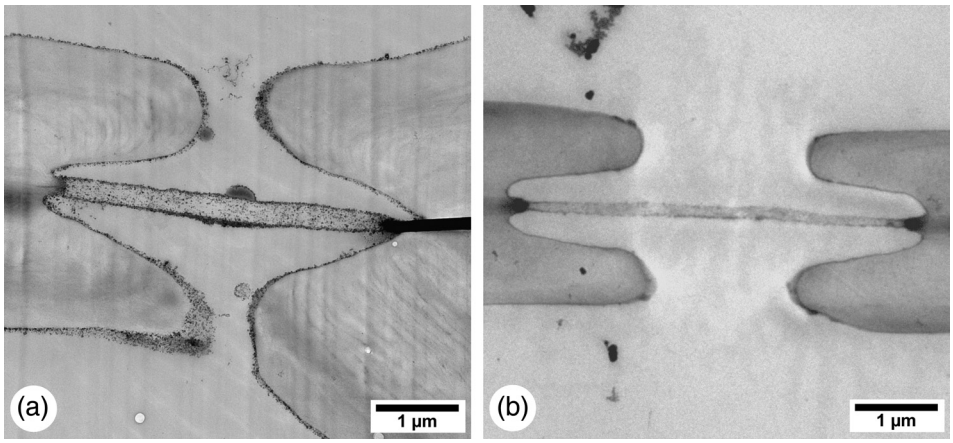

Figure 4. TEM image of bordered pits between two neighboring vessels in *P. cerasus* showing a thicker pit membrane in a fresh (i.e., hydrated) sample (a) as compared with an air-dried pit membrane that was only partially hydrated during TEM preparation (b).

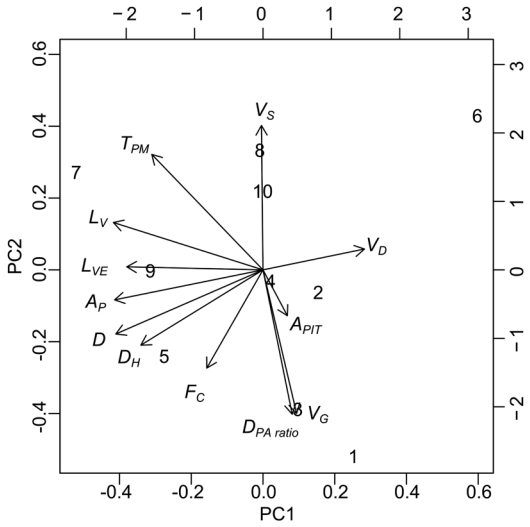

Figure 5. Principal component analysis of 12 wood anatomical traits on the first 2 principal component axes. Numbers represent P_{50} values, with 1 representing the least ($P_{50} = -3.54$ MPa) and 10 ($P_{50} = -6.26$ MPa) the most negative value. T_{PM} was based on air-dried material ($T_{PM\ dry}$).

Table 3. PCA eigenvalue factor loadings and *P* and *r* values of the correlation analysis of PCs and P_{50} (bold when $P < 0.05$); components with an eigenvalue >1 were retained; acronyms according to Table 1.

	PC1	PC2	PC3	PC4
Eigenvalue	4.312	3.34	2.14	1.00
% of variance	35.93	27.86	17.90	8.36
Cumulative %	35.93	63.79	81.69	90.03
D_H	0.886			
L_V	0.792			
V_D	−0.776			
D	0.776	0.511		
F_C		0.851		
A_P	0.459	0.846		
L_{VE}		0.730	−0.447	
A_{PIT}	−0.426	0.660	0.461	
$D_{PA\ ratio}$			0.925	
T_{PM}			−0.859	
V_S				0.968
V_G				−0.942
r	−0.325	0.128	0.431	**−0.735**
P	0.360	0.724	0.231	**0.015**

data of 97 species. According to these authors, intervessel connectivity allows species to achieve a higher specific hydraulic conductivity, but at the cost of increased vulnerability to embolism. However, owing to the lack of hydraulic conductivity data, it is unclear how cavitation resistance scales with hydraulic conductivity within the *Prunus* species studied. Contrary to our study, Martínez-Vilalta et al. (2012) used theoretical P_{50} values based on their hydraulic model instead of experimental data. Moreover, these authors applied a point pattern analysis instead of determining vessel-grouping indices (V_G, V_S) according to Carlquist (1984). The point patterns analysis method is based on various theoretical models explaining the presence of point to point interactions for describing the spatial distribution (aggregation and grouping) of xylem conduits (Bivand et al. 2009, Mencuccini et al. 2010).

To what extent do our data support the vessel-grouping hypothesis of Carlquist (1984)? Contrary to data on *Acer* (Lens et al. 2011), the results from this study do not provide support for Carlquist's vessel-grouping hypothesis. Carlquist (1984, 2001, 2009) suggested that vessels show a tendency toward an increase in vessel grouping in xeric environments, but a mainly solitary vessel arrangement in more mesic areas. His functional explanation was that vessel multiples may provide alternative, redundant pathways when some vessels become embolized. Carlquist's hypothesis, however, is restricted to species with non-conductive imperforate tracheary elements (ITEs), because tracheids (especially vasicentric tracheids) would provide an additional hydraulic pathway to the vessel

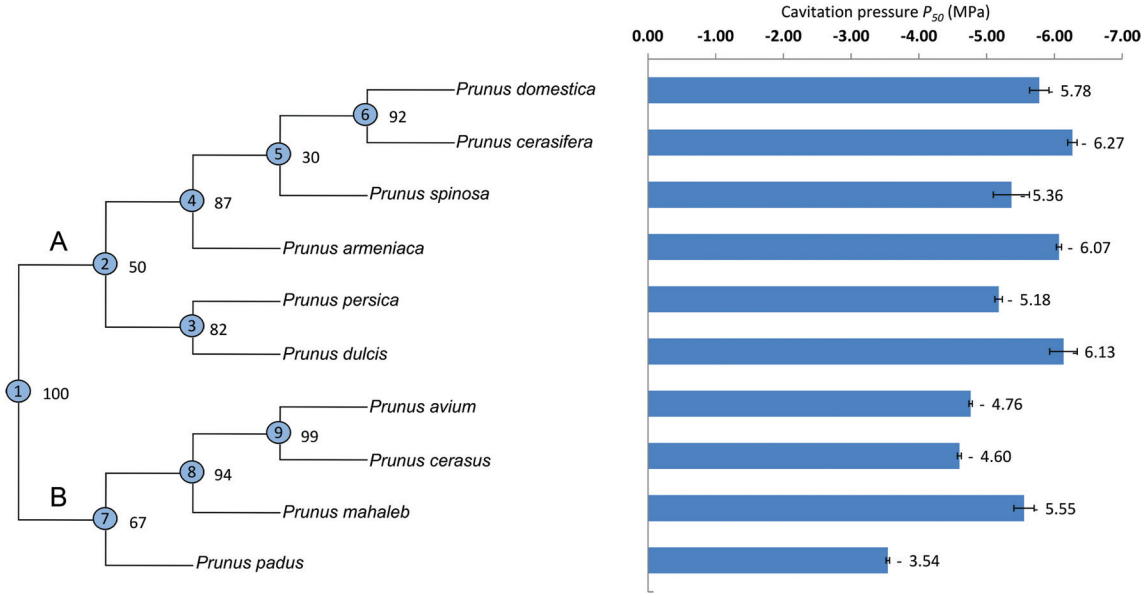

Figure 6. Phylogenetic tree based on the ITS and the trnL–trnF sequences for 10 *Prunus* species; A and B illustrate two major clades; node numbers are given with bootstrap support values; P_{50} values (MPa, ±SE) are shown on the right.

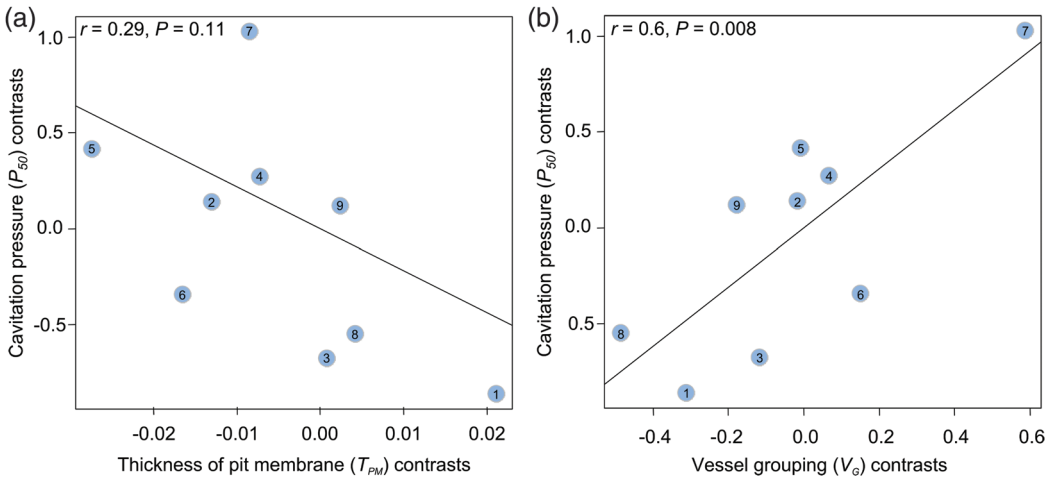

Figure 7. Phylogenetically independent contrasts for the 10 *Prunus* species studied. Numbers correspond to the node numbers given in Figure 6, showing the PICs calculated between P_{50} and dry intervessel pit membrane thickness ($T_{PM\ dry}$) (a), and between P_{50} and vessel-grouping index (V_G) (b).

network, making any tendency toward increased vessel grouping redundant in dry environments (Carlquist 1984, Sano et al. 2011). Careful observation of macerated wood samples showed that tracheids did not occur in the 10 *Prunus* species studied, which is in line with Carlquist's (1985) observation that tracheids are absent in deciduous species of *Prunus*. Moreover, TEM observations of bordered pits in ITEs of *Prunus* frequently showed perforated pit membranes, which also indicate a non-conductive nature in the species studied (Sano et al. 2011). Even so, tracheids do not seem to have a great impact on cavitation resistance in various Rosaceae (Hacke et al. 2009).

Moreover, care should be taken when linking the vessel-grouping hypothesis with P_{50} values, because Carlquist's grouping hypothesis refers to the correlation between vessel grouping and soil moisture availability, without quantifying cavitation resistance of the xylem. It is now clear that P_{50} values and, for instance, mean annual precipitation (MAP) are decoupled in many cases: depending on the whole-plant hydraulic strategy, species with a wide range of P_{50} values co-occur at the same site, and species with similar P_{50} values grow in areas with contrasting MAP (Maherali et al. 2004, Choat et al. 2012). Considering the moisture availability of the sites where we collected our 10 *Prunus* species, we note that *P. mahaleb* and *P. padus*, which were the only species collected at a xeric and humid site, respectively, clearly showed the lowest (*P. mahaleb*) and the highest (*P. padus*) vessel-grouping index. This finding is thus the opposite of what would be expected

based on Carlquist's grouping hypothesis, although certainly more species from dry and wet environments should be considered before any generalization can be made, ideally considering the whole-plant hydraulic performance.

Our data illustrate that the variation in P_{50} in *Prunus* is not influenced by the total intervessel pit membrane surface area per vessel, as was demonstrated in the correlation analysis (A_P; $r = -0.18$, $P = 0.6$) and the PCA (Table 3). A possible explanation on why our data do not confirm the rare-pit hypothesis could be the relatively narrow range in P_{50} (2.7 MPa) across the 10 *Prunus* species studied. In order to evaluate the relationship between A_P and P_{50} in a broader context, we used the literature data to compare our *Prunus* dataset with other Rosaceae and angiosperms, including diffuse-porous and ring-porous species (Figure 8). While the negative scaling between A_P and P_{50} remains clearly significant, this dataset ($n = 86$ species) suggests that the rare pit hypothesis is weaker ($r^2 = 0.37$) than previously reported based on smaller datasets (Wheeler et al. 2005, Hacke et al. 2006). Cai and Tyree (2010) noticed that these earlier regressions of P_{50} versus A_P are close to the r^2 of P_{50} versus vessel diameter. However, if the rare pit hypothesis is correct, P_{50} values should correlate more strongly with A_P than the vessel diameter. Data on the hydraulically weighted diameter (D_H) for a subset of the species plotted in Figure 8 ($n = 59$) suggest that D_H shows no correlation with P_{50} ($r^2 = 0.07$), which is surprising, but in support of the rare pit hypothesis.

An alternative explanation why our *Prunus* dataset does not support the rare pit hypothesis as expected is that the frequency of large leaky pits may not only depend on tissue-level characteristics (e.g., pit membrane area) but also on pit-level properties (Choat and Pittermann 2009). The dry pit membrane thickness values were significantly correlated with P_{50} ($T_{PM\ dry}$, $r = -0.79$, $P = 0.01$), and weaker correlations were found for the wet pit membrane thickness and pit aperture shape. Our finding that wet pit membranes are 44% thicker than dried pit membranes illustrates that pit membrane structure is strongly affected by drying, a finding that had been suggested previously (Jansen et al. 2008). However, high intra-tree variability was noticed for T_{PM} in all species, with average standard deviations of 25%. The overall range in $T_{PM\ wet}$ between the 10 species was relatively low (i.e., <150 nm) compared with the 254 nm observed for a 2 MPa P_{50} range by Lens et al. (2011), and could be associated with the low interspecific variability in intervessel wall thickness (Jansen et al. 2009). Plavcová et al. (2011) showed that differing light conditions can alter the pit membrane thickness in hybrids of poplar. Correlations between cavitation resistance and pit membrane thickness have also been reported by Jansen et al. (2009), Lens et al. (2011) and within plants of *Helianthus annuus* L. that were cultivated under contrasting irrigation and nutrient regimes (Scholz et al., unpublished data). Given the consistent thickness of microfibrils in pit membranes across species, pit membrane thickness is likely to reflect the number of microfibril layers in a pit membrane, which seems tightly linked with the size of the pit membrane pores and air-seeding pressure (Choat et al. 2004, Jansen et al. 2009). Our finding that more elliptical pit apertures are associated with higher cavitation resistance is in agreement with Lens et al. (2011). Thus, vessels that show bordered pits with an elliptical aperture and a thick membrane show higher cavitation resistance. The lack of any correlation in our data between P_{50} and intervessel wall thickness, as previously suggested by Cochard et al. (2008) for exactly the same species, is remarkable. A possible explanation could be that in the present study only the wall thickness in the middle was measured, excluding cell corners of adjacent vessels. Moreover, our data were based on five samples per species and 25 measurements per sample, instead of 60 measurements from a single sample per species.

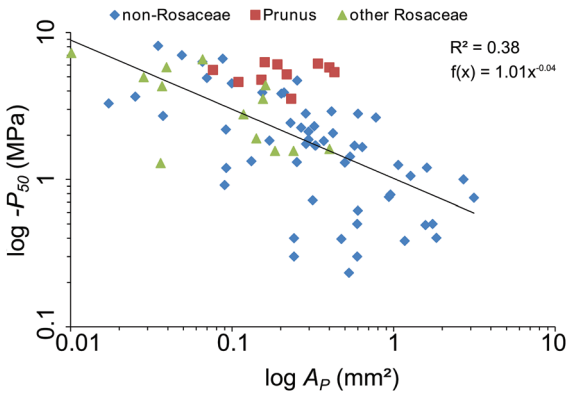

Figure 8. P_{50} (absolute values were taken for the log scaling) versus pit membrane surface area (A_P) for the 10 *Prunus* species studied. Data for additional Rosaceae and angiosperms were taken from Wheeler et al. (2005), Hacke et al. (2006, 2009), Sperry et al. (2007), Christman et al. (2009) and Lens et al. (2011). The regression line is shown for all species ($n = 86$).

Furthermore, there is no direct and clear evidence that an increase in the number of intervessel pits, and thus in the total intervessel pit membrane area per vessel (A_P), automatically increases the likelihood of a large pit pore that triggers air-seeding (Choat et al. 2003). However, quantifying pit membrane porosity remains problematic despite the application of a wide range of techniques (Choat et al. 2003, 2004, 2008).

The comparative phylogenetic analyses support the idea that the adaptation to cavitation resistance has co-evolved in closely related species of *Prunus*, with only *P. mahaleb* as an exception in clade B (Figure 6). Owing to its very small vessel diameter ($D_{P.\ mahaleb} = 15.5$ µm; $D_{\text{all species}} = 20$ µm), its high vessel density ($V_{D_{P.\ mahaleb}} = 70.77$ vessels mm^{-2}; $V_{D_{\text{all species}}} = 40.18$ vessels mm^{-2}) and its pronounced diffuse-porous wood, this species has a unique anatomical structure compared with the other species, which probably reflects the xerophilic site where *P. mahaleb* was collected. Evolutionary changes detected between F_{PF} and P_{50}

were not supported in the correlation analysis, suggesting that evolutionary changes of F_{PF} happened in different directions.

In conclusion, cavitation resistance across the *Prunus* species studied is determined by a series of interconnected characters related to the spatial distribution of the vessel network, especially vessel-grouping index (V_G), solitary vessel index (V_S) and vessel contact length fraction (F_{LC}), in addition to qualitative pit characteristics such as pit membrane thickness (T_{PM}) and pit aperture shape ($D_{PA\ ratio}$). Co-evolution was shown for vessel connectivity features, but not for pit membrane thickness (T_{PM}) and pit aperture shape ($D_{PA\ ratio}$). This suggests that vessel connectivity traits have evolved together with cavitation resistance in *Prunus*. Further empirical and comparative works on the plasticity of quantitative and qualitative wood anatomical features are needed in combination with phylogenetic and evolutionary analyses to better understand the mechanisms of cavitation resistance at an intraspecific, interspecific and intra-tree level (Fonti and Jansen 2012, Schulte 2012, von Arx et al. 2012).

Supplementary data

Supplementary data for this article are available at *Tree Physiology* Online.

Acknowledgments

We acknowledge U. Burrett, N. Möbius and S. Fiedler for technical assistance with lab work and image analysis, S. Janssens (KU Leuven) for the phylogeny reconstruction, S. Stuart (MacQuarie University) for phylogenetic comparative analyses, F. Lens (Leiden University) for valuable discussions and anonymous reviewers for useful comments and suggestions.

Conflict of interest

None declared.

Funding

This study was financially supported by the 'Juniorprofessorenprogramm' from the Ministry of Science, Research, and the Arts of Baden-Wurttemberg (Germany).

References

Ackerly DD (2000) Taxon sampling, correlated evolution, and independent contrasts. Evolution 54:1480–1492.

Bhaskar R, Valiente-Banuet A, Ackerly DD (2007) Evolution of hydraulic traits in closely related species pairs from Mediterranean and non-Mediterranean environments of North America. New Phytol 176:718–726.

Bivand R, Pebesma E, Gómez-Rubio V (2009) Applied spatial data analysis with R. 1st edn. Springer, New York.

Bortiri E, Oh S-H, Jiang J, Baggett S, Granger A, Weeks C, Buckingham M, Potter D, Parfitt DE (2001) Phylogeny and systematics of *Prunus* (Rosaceae) as determined by sequence analysis of ITS and the chloroplast trnL–trnF spacer DNA. Syst Bot 26:797–807.

Brodersen CR, Lee EF, Choat B, Jansen S, Phillips RJ, Shackel KA, McElrone AJ, Matthews MA (2011) Automated analysis of three-dimensional xylem networks using high-resolution computed tomography. New Phytol 191:1168–1179.

Brodribb TJ, Cochard H (2009) Hydraulic failure defines the recovery and point of death in water-stressed conifers. Plant Physiol 149:575–584.

Brodribb TJ, Bowman DJMS, Nichols S, Delzon S, Burlett R (2010) Xylem function and growth rate interact to determine recovery rates after exposure to extreme water deficit. New Phytol 188:533–542.

Cai J, Tyree MT (2010) The impact of vessel size on vulnerability curves: data and models for within-species variability in saplings of aspen, *Populus tremuloides* Michx. Plant Cell Environ 33:1059–1069.

Carlquist S (1980) Further concepts in ecological wood anatomy, with comments on recent work in wood anatomy and evolution. Aliso 9:499–553.

Carlquist S (1984) Vessel grouping in dicotyledon wood: significance and relationship to imperforate tracheary elements. Aliso 10:505–525.

Carlquist S (1985) Vasicentric tracheids as a drought survival mechanism in the woody flora of southern California and similar regions. Aliso 11:37–68.

Carlquist S (2001) Comparative wood anatomy—systematic, ecological, and evolutionary aspects of dicotyledon wood. 2nd edn. Springer, Berlin, p 418.

Carlquist S (2009) Xylem heterochrony: an unappreciated key to angiosperm origin and diversifications. Bot J Linn Soc 161:26–65.

Choat B, Pittermann J (2009) New insights into bordered pit structure and cavitation resistance in angiosperms and conifers. New Phytol 182:557–560.

Choat B, Ball M, Luly J (2003) Pit membrane porosity and water stress-induced cavitation in four co-existing dry rainforest tree species. Plant Physiol 131:41–48.

Choat B, Jansen S, Zwieniecki MA, Smets E, Holbrook NM (2004) Changes in pit membrane porosity due to deflection and stretching: the role of vestured pits. J Exp Bot 55:1569–1575.

Choat B, Sack L, Holbrook NM (2007) Diversity of hydraulic traits in nine *Cordia* species growing in tropical forests with contrasting precipitation. New Phytol 175:686–698.

Choat B, Cobb AR, Jansen S (2008) Structure and function of bordered pits: new discoveries and impacts on whole-plant hydraulic function. New Phytol 177:608–625.

Choat B, Jansen S, Brodribb TJ et al. (2012) Global convergence in the vulnerability of forests to drought. Nature 491:752–755.

Christman MA, Sperry JS, Adler FR (2009) Testing the 'rare pit' hypothesis for xylem cavitation resistance in three species of *Acer*. New Phytol 182:664–674.

Christman MA, Sperry JS, Smith DD (2012) Rare pits, large vessels and extreme vulnerability to cavitation in a ring-porous tree species. New Phytol 193:713–720.

Cochard H, Damour G, Bodet C, Tharwat I, Poirier M, Améglio T (2005) Evaluation of a new centrifuge technique for rapid generation of xylem vulnerability curves. Physiol Plant 124:410–418.

Cochard H, Barigaha ST, Kleinhentz M, Eshelc A (2008) Is xylem cavitation resistance a relevant criterion for screening drought resistance among *Prunus* species? J Plant Physiol 165:976–982.

Davis SD, Ewers FW, Sperry JS, Portwood KA, Crocker MC, Adams GC (2002) Shoot dieback during prolonged drought in *Ceanothus* (Rhamnaceae) chaparral of California: a possible case of hydraulic failure. Am J Bot 89:820–828.

Delzon S, Douthe C, Sala A, Cochard H (2010) Mechanism of water-stress induced cavitation in conifers: bordered pit structure and

function support the hypothesis of seal capillary-seeding. Plant Cell Environ 33:2101–2111.
Drummond A, Ashton B, Buxton S et al. (2011) Geneious v5.4. http://www.geneious.com/.
Felsenstein J (1985) Phylogenies and the comparative method. Am Nat 125:1–15.
Fonti P, Jansen S (2012) Xylem plasticity in response to climate. New Phytol 195:734–736.
Franklin GL (1945) Preparation of thin sections of synthetic resins and wood-resin composites, and a new macerating method for wood. Nature 155:51–51.
Hacke UG, Jansen S (2009) Embolism resistance of three boreal conifer species varies with pit structure. New Phytol 182:675–686.
Hacke UG, Sperry JS, Wheeler JK, Castro Noval L (2006) Scaling of angiosperm xylem structure with safety and efficiency. Tree Physiol 26:689–701.
Hacke UG, Sperry JS, Feild TS, Sano Y, Sikkema EH, Pittermann J (2007) Water transport in vesselless angiosperms: conducting efficiency and cavitation safety. Int J Plant Sci 168:1113–1126.
Hacke UG, Jacobsen AL, Pratt R (2009) Xylem function of arid-land shrubs from California, USA: an ecological and evolutionary analysis. Plant Cell Environ 32:1324–1333.
Jansen S, Pletsers A, Sano Y (2008) The effect of preparation techniques on SEM-imaging of pit membranes. IAWA J 29:161–178.
Jansen S, Choat B, Pletsers A (2009) Morphological variation of intervessel pit membranes and implications to xylem function in angiosperms. Am J Bot 96:409–419.
Jansen S, Gortan E, Lens F, Lo Gullo MA, Salleo S, Scholz A, Stein A, Trifiló P, Nardini A (2011) Do quantitative vessel and pit characters account for ion-mediated changes in the hydraulic conductance of angiosperm xylem? New Phytol 189:218–228.
Karnovsky MJ (1965) A formaldehyde-glutaraldehyde fixative of high osmolality for use in electron microscopy. J Cell Biol 3:137–138.
Kembel S, Cowan P, Helmus M, Cornwell WK, Morlon H, Ackerly DD, Blomberg SP, Webb C (2010) Picante: R tools for integrating phylogenies and ecology. Bioinformatics 26:1463–1464.
Lamy J-B, Bouffier L, Burlett R, Plomion C, Cochard H, Delzon S (2011) Uniform selection as a primary force reducing population genetic differentiation of cavitation resistance across a species range. PloS ONE 6:e23476.
Lens F, Sperry JS, Christman MA, Choat B, Rabaey D, Jansen S (2011) Testing hypotheses that link wood anatomy to cavitation resistance and hydraulic conductivity in the genus *Acer*. New Phytol 190:709–723.
Lens F, Tixier A, Cochard H, Sperry JS, Jansen S, Herbette S (2013) Embolism resistance as a key mechanism to understand adaptive plant strategies to drought. Curr Opin Plant Biol 16:287–292.
Loepfe L, Martínez-Vilalta J, Piñol J, Mencuccini M (2007) The relevance of xylem network structure for plant hydraulic efficiency and safety. Am J Bot 247:788–803.
Maherali H, Pockman WT, Jackson RB (2004) Adaptive variation in the vulnerability of woody plants to xylem cavitation. Ecology 85:2184–2199.
Martínez-Cabrera HI, Jones CS, Espino S, Schenk HJ (2009) Wood anatomy and wood density in shrubs: responses to varying aridity along transcontinental transects. Am J Bot 96:1388–1398.
Martínez-Vilalta J, Mencuccini M, Alvarez X, Camacho J, Loepfe L, Piñol J (2012) Spatial distribution and packing of xylem conduits. Am J Bot 99:1–8.
McDowell NG, Pockman WT, Allen CD et al. (2008) Mechanisms of plant survival and mortality during drought: why do some plants survive while others succumb to drought? New Phytol 178:719–739.
Mencuccini M, Martínez-Vilalta J, Piñol J, Loepfe L, Burnat M, Alvarez X, Camacho J, Gil D (2010) A quantitative and statistically robust method for the determination of xylem conduit spatial distribution. Am J Bot 97:1247–1259.
Pittermann J, Choat B, Jansen S, Stuart S, Lynn L, Dawson T (2010) The relationships between cavitation safety and hydraulic efficiency in the pit membranes of conifers belonging to the Cupressaceae: the evolution of form and function. Plant Physiol 153:1919–1931.
Plavcová L, Hacke UG, Sperry JS (2011) Linking irradiance-induced changes in pit membrane ultrastructure with xylem vulnerability to cavitation. Plant Cell Environ 34:501–513.
R Core Team (2013) R: a language and environment for statistical computing. R Foundation for Statistical Computing, Vienna, Austria.
Rasband (1997) ImageJ. National Institutes of Health, Bethesda, MD, USA. http://rsb.info.nih.gov/ij/ (1 October 2011, date last accessed).
Rood SB, Patiño S, Coombs K, Tyree MT (2000) Branch sacrifice: cavitation-associated drought adaptation of riparian cottonwoods. Trees 14:248–257.
Sano Y, Morris H, Shimada H, Ronse De Craene LP, Jansen S (2011) Anatomical features associated with water transport in imperforate tracheary elements of vessel-bearing angiosperms. Ann Bot 107:953–964.
Schenk HJ, Espino S, Goedhart CM, Nordenstahl M, Martínez-Cabrera HI, Jones CS (2008) Hydraulic integration and shrub growth form linked across continental aridity gradients. Proc Natl Acad Sci USA 105:11248–11253.
Scholz A, Klepsch M, Karimi Z, Jansen S (2013) How to quantify conduits in wood? Front Plant Sci 4:56. doi:10.3389/fpls.2013.00056.
Schulte PJ (2012) Vertical and radial profiles in tracheid characteristics along the trunk of Douglas-fir trees with implications for water transport. Trees 26:421–433.
Sperry JS (2003) Evolution of water transport and xylem structure. Int J Plant Sci 164:115–127.
Sperry JS, Hacke UG, Wheeler JK (2005) Comparative analysis of end wall resistivity in xylem conduits. Plant Cell Environ 28:456–465.
Sperry JS, Hacke UG, Feild TS, Sano Y, Sikkema EH (2007) Hydraulic consequences of vessel evolution in angiosperms. Int J Plant Sci 168:1127–1139.
Stamatakis A (2006) RAxML-VI-HPC: maximum likelihood-based phylogenetic analyses with thousands of taxa and mixed models. Bioinformatics 22:2688–2690.
Stamatakis A, Ludwig T, Meier H (2005) RAxML-III: a fast program for maximum likelihood-based inference of large phylogenetic trees. Bioinformatics 21:456–463.
Tyree MT, Sperry JS (1989) Vulnerability of xylem to cavitation and embolism. Annu Rev Plant Biol 40:19–36.
Tyree MT, Zimmermann MH (2002) Xylem structure and the ascent of sap. 2nd edn. Springer, Berlin.
Von Arx G, Archer SR, Hughes MK (2012) Long-term functional plasticity in plant hydraulic architecture in response to supplemental moisture. Ann Bot 109:1091–1100.
Wheeler JK, Sperry JS, Hacke UG, Hoang N (2005) Inter-vessel pitting and cavitation in woody Rosaceae and other vesselled plants: a basis for a safety versus efficiency trade-off in xylem transport. Plant Cell Environ 28:800–812.
Wortemann R, Herbette S, Barigah TS, Fumanal B, Alia R, Ducousso A, Gomory D, Roeckel-Drevet P, Cochard H (2011) Genotypic variability and phenotypic plasticity of cavitation resistance in *Fagus sylvatica* L. across Europe. Tree Physiol 31:1175–1182.
Zanne AE, Westoby M, Falster DS, Ackerly DD, Loarie SR, Arnold SEJ, Coomes DA (2010) Angiosperm wood structure: global patterns in vessel anatomy and their relation to wood density and potential conductivity. Am J Bot 97:207–215.